Anisotropy and structural-defect contributions to percolative conduction in granular copper oxide superconductors

A. Díaz, J. Maza, and Félix Vidal
Laboratorio de Física de Materiales, Departamento de Física de la Materia Condensada, Universidad de Santiago de Compostela, 15706 Santiago de Compostela, Spain

(Received 5 February 1996; revised manuscript received 11 September 1996)

A well-defined temperature-independent slope of the current-voltage characteristics (CVC) is a common feature of granular high-temperature superconductors in the paracoherent state (grains superconducting; intergranular regions normal). By analyzing the contributions of anisotropy and structural defects to percolative conduction processes both in the normal state and in the paracoherent state, we quantitatively account for the observed CVC slopes using only the normal-state resistivity values. In particular, from effective-medium theory it is found that the CVC slope of nontextured granular $YBa_2Cu_3O_{7-\delta}$ (YBCO) should be equal to approximately one-third of the normal-state resistivity extrapolated to zero temperature. Simultaneous measurements of the CVC and normal-state resistivity on a batch of granular YBCO samples are also presented that verify our predictions with no free parameters. [S0163-1829(97)01902-4]

I. INTRODUCTION

Current-voltage characteristics (CVC) of polycrystalline high-temperature superconductors (HTS's) show a well-defined temperature- and low-field-independent slope for current in excess of the critical current, a fact known since soon after the discovery of HTS's.[1] In contrast, in low-temperature superconductors, the linear regime in the CVC takes place only in the mixed state, the slope being strongly temperature and field dependent, and has been interpreted as flux-flow dissipation.[2] The resistivity associated with the constant slope of CVC in copper oxides is commonly assigned to the intergrain junctions because they are the weakest links in the conduction path, the grain themselves going normal only at much higher current.[3] We will allude to that resistivity as the paracoherent resistivity ρ_p. However, the important physically relevant resistivity of polycrystalline materials for comparison with models or theories of junctions, weak-link networks, etc., is the (average) intergrain resistivity $\rho_{\rm wl}$ (wl stands for weak links). Since in the context of CVC only the intergrain network plays a role, it is tempting to identify $\rho_{\rm wl}$ with ρ_p, as has been in fact assumed in the literature.[4–6] In addition this resistance $\rho_{\rm wl}$ is taken simply as a free parameter, i.e., without trying any quantitative correlation with ρ_n, the measured normal-state resistivity.[7]

The objective of this work is to analyze, on the grounds of a simple empirical percolation model of granular superconductors, the relationship between $\rho_{\rm wl}$, ρ_p, and ρ_n and to provide then a quantitative explanation of the values measured for ρ_p in polycrystalline HTS's. We will show in particular that in contrast with the common assumption alluded to before, the resistivity of the average intergrain junction cannot be determined solely from the linear portion of the CVC. Identification of $\rho_{\rm wl}$ with ρ_p results, consequently, in an error. The importance of the proper interpretation of ρ_p cannot be minimized since it has been used, for instance, as a key ingredient to assess the validity of the theory of classical weak links to grain boundaries in HTS's.[4] Let us stress already here that the percolative nature of conduction caused by microcracks and other structural sample's defects acts on the real intergrain resistivity $\rho_{\rm wl}$ to yield a considerably larger apparent intergrain resistivity ρ_p. Paradoxically, the paracoherent resistivity ρ_p can be determined from the normal-state resistivity provided separation of inter- and intragrain contributions and proper analysis of percolative processes, especially the current distribution, are made. As a result, we will show that, for YBCO, ρ_p should be equal to approximately one-third of the normal-state resistivity extrapolated to zero temperature. Departure of the apparent intergrain resistivity ρ_p from the actual intergrain resistivity $\rho_{\rm wl}$ will be also correlated with the temperature slope of normal-state resistivity. The validity of our results will be confirmed by direct measurements of ρ_p on a batch of sintered $YBa_2Cu_3O_{7-\delta}$ (YBCO) samples, no free parameters being involved in the numerical comparison.

II. NORMAL AND PARACOHERENT PERCOLATIVE CONDUCTION

In this section we describe and parametrize the main mechanisms involved in the observed normal-state resistivity ρ_n, with both grains and grain junctions in the normal state, and also in the observed paracoherent resistivity ρ_p with the grains superconducting but the intergrain junctions still normal. We will especially focus on the percolative factors that control the effective length and effective cross section of current paths.

A. Normal-state resistivity

In electrical normal-state conduction in granular samples, current path frustration and/or meandering of current may occur by two quite distinct mechanisms. One is associated with the orientational disorder of anisotropic grains.[8] It depends on the degree of texturization, and has its origin in the extreme anisotropy of the copper oxides, the in-plane resistivity ρ_{ab} being orders of magnitude less than the out-of-plane resistivity ρ_c.[9] The upper path in Fig. 1(b) marked in dark gray is an example of current frustration by grain mis-

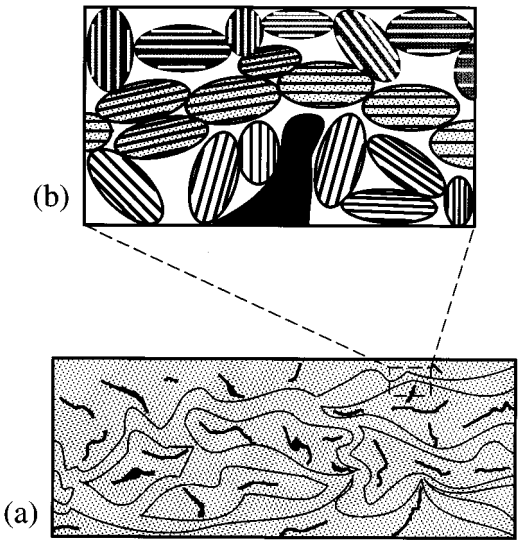

FIG. 1. Sketch of a granular HTS sample showing (a) the meandering (lengthening and shrinking) of current paths caused by cracks and (b) a finer scale view. In the latter, the channel in light gray corresponds to a conducting normal-state path due to the good alignment of the grains. In contrast, the grains in dark gray form a nonconducting channel in the normal state due to the grains' misalignment (see the 90° tilt grain boundaries), while in the paracoherent state this channel is a conducting one because of the loss of anisotropy ($\rho_{ab}=\rho_c=0$). Finally, the lower part of (b) is not conducting due to structural defects (cracks, not connected grains).

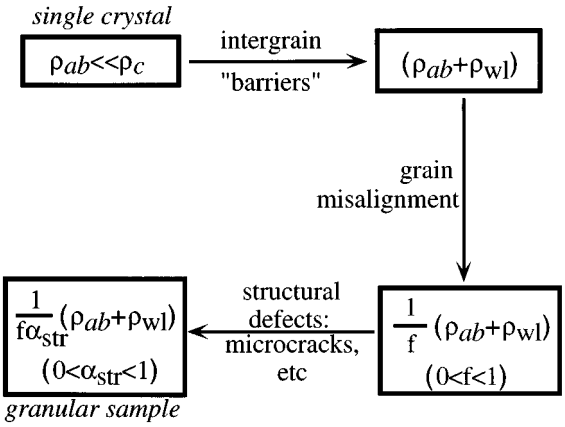

FIG. 2. Main underlying mechanisms of resistivity enhancement in granular samples starting from the resistivity of crystallites (see text for details).

alignment. Since we are assuming, because of the extreme conduction anisotropy, a total current blockage along pathways with misaligned grains, the current percolates through the sample along unobstructed paths, entailing a cross-section reduction and path lengthening[10] that increases resistivity by a multiplicative factor that we will denote as $1/f(0<f\leqslant 1)$. A distinct source of (apparent) resistivity enhancement comes from structural defects, from those on the scale on grains, as pores or isolating boundaries, to those on the scale of the sample, as microcracks. Figure 1 illustrates possible actual current paths (in light gray in the magnified view). The corresponding effect on resistivity by the latter quality-dependent factor will be written as $1/\alpha_{\rm str}$ $(0<\alpha_{\rm str}\leqslant 1)$. Besides the percolative processes, a series contribution to resistivity stemming from the intergrain ''barriers'' is to be added. This contribution is but the (average) intergrain resistivity $\rho_{\rm wl}$ mentioned in the Introduction.

Figure 2 summarizes in a flow-chart style the main steps in ''constructing'' the observed resistivity that we write accordingly as

$$\rho_n=\frac{1}{\alpha_n}\,(\rho_{ab}+\rho_{\rm wl}), \tag{1}$$

where α_n is a shorthand for

$$\alpha_n=f\alpha_{\rm str}, \tag{2}$$

and it may be referred to as the normal-state percolative factor. Note that $0<\alpha_n\leqslant 1$.

Approximations in the line of Eq. (1) have been successfully used in the study of fluctuation-induced conductivity in small metal particles,[11] dc conductivity,[12] paraconductivity,[13] and critical currents in granular copper oxides.[14] Our main contribution with respect to the aforementioned studies is the separation [cf. Eq. (2)] of sample-dependent effects (structural factor $\alpha_{\rm str}$) from essentially sample-independent effects (grain's misalignment or anisotropy factor f). We will see later that for nontextured samples f is indeed very weakly sample dependent. This splitting will manifest itself as a useful means to arrive at our final objective of accounting for the well-defined slope in CVC found in polycrystalline copper oxide superconductors.

The normal-state resistivity of polycrystalline (well-oxygenated) HTS's is linear in temperature. This linearity of ρ_n enables determination of the two sample parameters α_n and $\rho_{\rm wl}$. More precisely, on taking temperature derivatives in Eq. (1) and assuming $\rho_{\rm wl}$ constant[4,15] one gets

$$\alpha_n=\frac{\rho'_{ab}}{\rho'_n}, \tag{3}$$

where the primes stand for temperature derivatives. Similarly, from Eqs. (1) and (3)

$$\rho_{\rm wl}=\frac{\rho'_{ab}}{\rho'_n}\,\rho_n(0)=\alpha_n\rho_n(0), \tag{4}$$

where $\rho_n(0)$ is the extrapolation of the normal-state resistivity to zero temperature, or simply the zero-intercept resistivity. In writing Eq. (4), ρ_{ab} is assumed, based on single-crystal measurements,[16] to vary linearly with temperature ($\rho'_{ab}=0.5\ \mu\Omega\,{\rm cm\,K^{-1}}$) with a negligible zero-temperature intercept. For typical polycrystalline Y-based HTS's α_n is in the range 0.2–0.05 and $\rho_{\rm wl}$ in the range 15–400 $\mu\Omega$ cm (see also Table I). It is worth noting the low values of α_n (in the ideal case $\alpha_n=1$), but also the fact that the intergrain resistivity contribution $\rho_{\rm wl}$ is of the same order of magnitude as the intragrain contribution: $\rho_{ab}(100\ {\rm K})\approx 50\ \mu\Omega\,{\rm cm}$. Note that the situation is quite different for low-temperature superconductors. In that case the array of (Josephson) junctions may be fabricated by pressing together bulk metallic grains in a matrix. Because one deals with good conducting isotro-

TABLE I. Relevant parameters of the specimens used in this work (see text for details).

Sample	T_{ci} (K)	ρ_{wl} ($\mu\Omega$ cm)	α_n	$\rho_n(0)$ ($\mu\Omega$ cm)	$f\rho_n(0)$ ($\mu\Omega$ cm)	ρ_p ($\mu\Omega$ cm)
Y16D6a	91.2	370	0.087	4260	1420	1200
Y16D2a	91.4	65.6	0.064	1030	343	310
Y16D2d	91.2	18.9	0.144	130	43	50

pic grains, the normal resistance of the junctions is simply the measured resistance of the assembly.[17]

B. Paracoherent state

Below the transition temperature and for a high enough current level (greater than the critical current of intergrain junctions but not high enough to force the transition of the grains themselves) an ohmic regime is reached. The main difference between percolation in the normal state and in this paracoherent state is that in the latter the orientational disorder is irrelevant as the grain resistivity becomes vanishingly small both in the ab plane and the c direction, resulting in the loss of anisotropy. As an example consider again the upper current path drawn in dark gray in Fig. 1(b). It is prohibited in the normal state since current cannot flow along the c direction because of the extreme anisotropy. Nevertheless, once bulk grains go superconducting (but the intergrain junctions remain normal), nothing hinders conduction along that path. In sum, only the structural quality factor α_{str} and the intergrain resistivity ρ_{wl} enter the paracoherent resistivity ρ_p, i.e.,

$$\rho_p = \frac{1}{\alpha_{str}}\,\rho_{wl}, \tag{5}$$

a relationship which through Eqs. (2) and (4) may also be recast as

$$\rho_p = f\rho_n(0). \tag{6}$$

Figure 3 further illustrates the various resistivities involved in the analysis. Note the sequence $\rho_n(0) > \rho_p > \rho_{wl}$.

In light of Eq. (5), it is easy to see that the crude approximation often made (see Sec. I) $\rho_p = \rho_{wl}$ is incorrect, i.e., in general $\alpha_{str} < 1$. This is because structural defects (cracks, etc.) obviously remain as path-frustrating mechanisms even with the grains superconducting. A possible better approximation is to set $\rho_{ab} = 0$ in Eq. (1), i.e., $\alpha_{str} = \alpha_n$. Again, this involves a conceptual error as grain misalignment restricts current flow with the whole sample in the normal state but not when the grains are in the superconducting state, as singled out above. With this notation, this means $\alpha_n \leqslant \alpha_{str}$, equality applying only for an (ideal) perfectly textured sample.

Prediction of values for the apparent intergrain resistivity ρ_p requires knowledge of f and $\rho_n(0)$ as conveyed by Eq. (6). The latter is readily obtained from normal-state measurements. Only the factor f, namely the resistivity enhancement by the combination of anisotropy plus grain misalignment, is left. A main contribution of this work is precisely to work out an expression for f on the grounds of the effective-medium theory. This is done in the next section.

III. ANISOTROPY-INDUCED RESISTIVITY ENHANCEMENT

Effective-medium theory (EMT), as applied to the study of the heterogeneous media, intends to find a homogeneous medium having the same overall properties as the original composite medium. Inhomogeneity, always understood as macroscopic inhomogeneity, may include multiphase media but also single-phase anisotropic materials in polycrystalline form. Granular copper oxides, and in particular the $YBa_2Cu_3O_{7-\delta}$ (YBCO) family we will focus on, belong to the latter category. Although a general formulation of EMT for anisotropic media exists,[18] application of it to our particular case would be much less transparent and cumbersome than the ''first-principles calculation'' we work out here.

In order to perform calculations on the grounds of the EMT, we must first model granular (nontextured) HTS's in some manageable but realistic way. Among the different simple geometrical forms one can choose in modeling the grains, we have selected an oblate ellipsoid (Fig. 4). There are several physical reasons that support this choice, the principal one being the preferred growth along the ab plane of HTS systems as observed in single crystals and in SEM photographs of polycrystalline samples. Moreover, in an oblate ellipsoid, the a and b axes are geometrically equivalent, a fact that agrees with their established equivalence in the

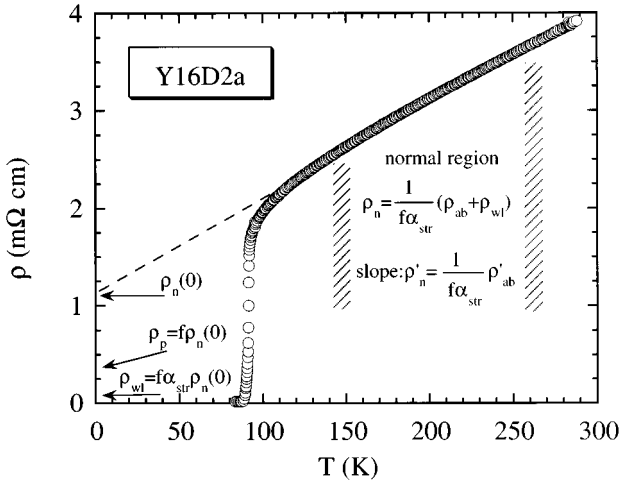

FIG. 3. Schematic figure showing the main resistivities involved in this work on a typical resistivity vs temperature curve for a granular superconductor. $\rho_n(0)$ is the extrapolation to zero temperature of the normal-state resistivity ρ_n, ρ_p is the resistivity of the paracoherent state (grains superconducting; intergranular regions normal), ρ_{wl} is the average intergrain resistivity (wl stands for weak links), and ρ_{ab} is the intragrain in-plane resistivity. The other two relevant parameters are the structural factor α_{str} accounting for porosity, microcracks, etc., and the anisotropy factor f arising from the anisotropy and misalignment of grains ($\alpha_{str}, f < 1$).

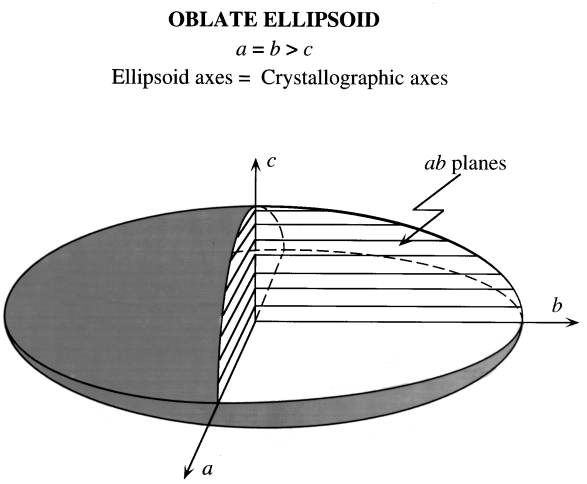

FIG. 4. Geometry of a HTS anisotropic grain used in this work. Note the ab HTS planes stacked in parallel to the ab sections of the oblate ellipsoid.

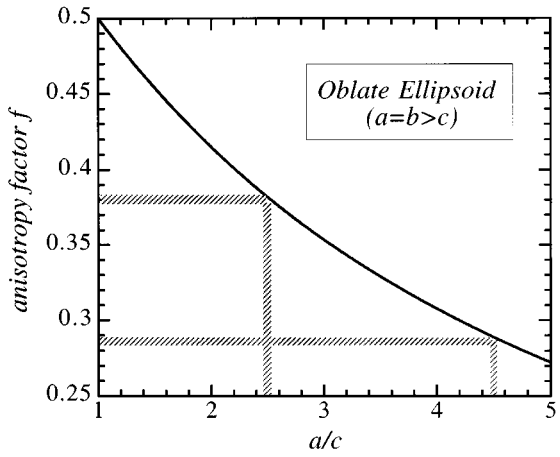

FIG. 5. Resistivity enhancement factor f due to the combination of grain misalignment and anisotropy calculated on the grounds of the effective-medium theory. a/c is the mean aspect ratio of the grains. As can be seen, f is only weakly dependent on a/c. In particular, for a typical variation of a/c in $YBa_2Cu_3O_{7-\delta}$ between 2.5 and 4.5, f ranges only from 0.38 to 0.29 (dashed bars).

physical properties of copper oxide HTS's. In sum, polycrystalline HTS's (and in particular, YBCO) is modeled as consisting of grains taken as oblate ellipsoids, their principal axes coinciding with the crystallographic axes, with a mean aspect ratio c/a and random orientations.

Consider an ellipsoidal grain in the heterogeneous medium surrounded by all other grains that one assumes are replaced by an equivalent homogeneous medium of unknown conductivity $\sigma_{\rm eff}$. Let $\mathbf{J}^{\rm in}$ be the current density through the reference grain when an electric field $\mathbf{E}$ is applied to the composite medium, and $\mathbf{J}_{\rm eff}$ be the current density that would flow through the homogeneous medium only. Since the homogeneous medium represents a spatial average, the average of $\mathbf{J}^{\rm in}$ over all possible orientations of the reference grain, denoted as $\langle \mathbf{J}^{\rm in} \rangle$, should also give $\mathbf{J}_{\rm eff}$, i.e.,

$$\langle \mathbf{J}^{\rm in} \rangle = \mathbf{J}_{\rm eff} = \sigma_{\rm eff} \mathbf{E}. \tag{7}$$

This is the main statement of the EMT. The calculation of $\mathbf{J}^{\rm in}$ or equivalently the electric field $\mathbf{E}^{\rm in}$ within the ellipsoid under the applied field $\mathbf{E}$ is a classical textbook result[19]

$$E_j^{\rm in} = \left[1 + \frac{n_j}{\sigma_{\rm eff}} (\sigma_j^{\rm in} - \sigma_{\rm eff}) \right]^{-1} E_j, \quad \text{with } j = x,y,z, \tag{8}$$

where $\sigma_j^{\rm in}$ are the principal values σ_a, σ_b, and σ_c of the conductivity tensor and the n_j are the so-called depolarization coefficients, whose principal values for an oblate ellipsoid are given by[19]

$$\begin{aligned} n_{33} = n_z &= \frac{1+e^2}{e^3} (e - \arctan e), \\ n_{11} = n_{22} = n_x = n_y &= \frac{1}{2} (1 + n_z), \end{aligned} \tag{9}$$

where e is the eccentricity of the oblate ellipsoid given by $e = \sqrt{(a/c)^2 - 1}$. The main condition (7) is written now, by Eq. (8), as

$$\sigma_{\rm eff} = \left\langle \left[1 + \frac{n_j}{\sigma_{\rm eff}} (\sigma_j^{\rm in} - \sigma_{\rm eff}) \right]^{-1} \sigma_j^{\rm in} \right\rangle. \tag{10}$$

In our particular case this calculation is greatly simplified because $\sigma_a \approx \sigma_b \gg \sigma_c$.[9] After some straightforward algebra, and denoting $\sigma_{ab} \equiv \sigma_a \simeq \sigma_b$, one arrives at the expression

$$\sigma_{\rm eff} = \frac{3n_z - 3}{3n_z - 5} \sigma_{ab}. \tag{11}$$

The factor in Eq. (11) represents the resistivity enhancement due only to the combination of grain anisotropy plus misalignment (random orientations), so it is directly the factor f in Eq. (2), i.e.,

$$f = \frac{3n_z - 3}{3n_z - 5}. \tag{12}$$

It can be said that the anisotropy contribution is a sample-dependent mechanism in that grain's eccentricity enters neatly the result in Eq. (12). This is not quite so. First, this dependence is a very weak one, as can be seen in Fig. 5, which is a plot of the anisotropy resistivity factor f as a function of the aspect ratio of grains. Second, by simply estimating aspect ratios from many granular YBCO through SEM micrographs published in the literature as well as from our own samples, we have verified that the range spanned is less than may be thought in advance: Most aspect ratios are between 2.5 and 4.5. This is the x-axis band drawn in Fig. 5. The important result is that the corresponding y-axis band greatly narrows and ranges only from 0.28 to 0.38. In sum, we conclude that as a rule of thumb for YBCO to within about 20%, we can take the value 1/3 for the factor f.

An interpretation of this number in light of Eqs. (2) and (3) is pertinent. We are saying that for a nontextured granular, but otherwise structurally perfect, HTS sample (no pores, microcracks, other phases, ...) $\alpha_{\rm str} = 1$ and $f \approx 1/3$ so that $\alpha_n \approx 1/3$ by Eq. (2). From Eq. (3), $\rho_n' \simeq 3\rho_{ab}'$, i.e., this ideal sample should have a temperature slope of resistivity about three times that of single crystals, i.e., around 1.5 $\mu\Omega$ cm K^{-1}.

Based on the preceding discussion, the question naturally arises as to the existence of granular samples of such high quality that they have resistivity slopes this low. The answer can come only from experiment: when studying dc conductivity in nontextured oxide cuprates Halbritter and collaborators (Ref. 12) came across a subgroup of samples whose (temperature) resistivity slopes clustered at about 1.8 $\mu\Omega$ cm K^{-1}, which is 3.6 times that of single crystal, and also had very low zero-intercept resistivities. As a further natural check, we have looked into our own resistivity data bank to find that the lowest slope value was 1.66 $\mu\Omega$ cm K^{-1}, i.e., 3.3 times the intrinsic resistivity slope of the ab plane (in this case, however, the zero-intercept resistivity had a medium value).

These two numerical examples can be brought to an even closer accord with our model estimates by realizing that, however structurally perfect those samples may be, some degree of porosity is surely present. We want then to substract the effect of porosity from the observed ρ_n' values so as to compare with the value of $\rho_n'=1.5$ $\mu\Omega$ cm K^{-1} for ideal samples. First-order correction for porosity may be obtained simply by applying the classical results for composite media one of which (air) is isolating (see, e.g., Ref. 19, Sec. 9). Denoting by $v_{\rm por}$ the volume fraction of voids, the correction to subtract the porosity contribution from the observed resistivity is $\rho\rightarrow\rho[1-3/2v_{\rm por}]^{-1}$. A very typical value for porosity is 10%, i.e., $v_{\rm por}=0.1$. Application of the above factor to the numerical examples leads to temperature slope factor changes of 3.6→3.1 and 3.3→2.8, which are yet closer to the expected value of 3.

There are then experimental and theoretical bases for the fact that when microcracks or other path-frustrating mechanisms, other than anisotropy, are absent, the observed temperature slope of resistivity in polycrystalline nontextured YBCO should be around (precision may be increased if the aspect ratio of grains is well known) three times that of the intrinsic ab-plane resistivity slope. This result, by Eq. (6), amounts to stating finally that the paracoherent resistivity ρ_p should equal one-third of the zero-intercept normal-state resistivity $\rho_n(0)$. Since both resistivities are easily measurable, the experimental check is obligatory and it is the content of the next section.

IV. EXPERIMENTAL VERIFICATION

At the end of the last section some suggestive evidence for the validity of our results was given. Here we want to use Eq. (6) to determine in $YBa_2Cu_3O_{7-\delta}$ the apparent intergrain resistivity ρ_p associated with the linear regime of CVC from normal-state resistivity and then make a comparison with the measured values.

The polycrystalline YBCO samples used for that purpose were prepared using the conventional ceramic process. Samples were sintered in air at 930 °C for 6–24 h and then annealed in pure oxygen at 350 °C for 6 h. Quality of the samples was verified by x-ray diffraction, which showed that they are single phase within 4%. The high values of the inflexion-point temperature of the resistivity transition (T_{ci} in Table I) provide an extra validation of their quality. Sample porosity as estimated from comparison with the YBCO density (6.36 g cm^{-3}) is around 10–15 %.

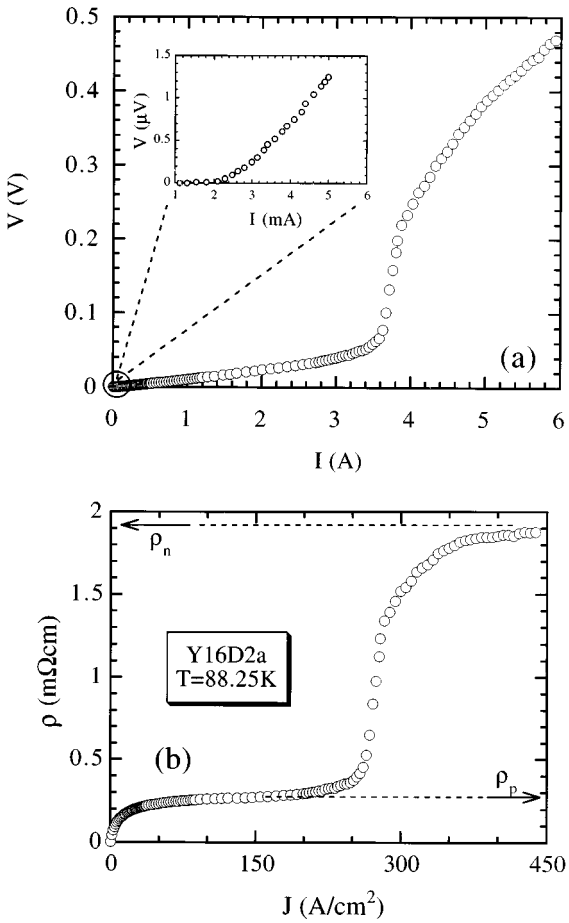

FIG. 6. (a) Complete current-voltage characteristics of one of the samples $YBa_2Cu_3O_{7-\delta}$ used in this work. Note the two linear regimes corresponding to junctions going normal (between a few mA and 3.5 A) and to the whole sample becoming normal ($I>4.5$ A). In the inset a detailed view of the intergrain transition is plotted. (b) Resistivity vs current density equivalent to curve (a). The two well-defined resistivity plateaus corresponding to the linear regimes of (a) are clearly shown. The lower plateau corresponds to a paracoherent resistivity $\rho_p=0.31$ mΩ cm. The value of 1.9 mΩ cm of the higher plateau agrees quite well with the value of 2.1 mΩ cm extrapolated from the normal-state resistivity to the actual $T=88.25$ K.

Contact pads were made by silver evaporation onto the samples. A subsequent annealing at 350° in O_2 atmosphere for 1 h reduced the contact resistivity to 10^{-5}–10^{-6} Ω cm^2 (typical contact area around 1 mm^2), which corresponds to high-quality contacts.[20] CVC curves were measured by using a specially designed cryostat that maintains the sample in a liquid-nitrogen bath, controlled in temperature by varying its vapor pressure. All these experimental precautions ensured that heating in the contacts due to the use of relatively high currents was negligible. Measurements were made with direct current.

Figure 6(a) shows the entire CVC for one of the YBCO samples. Notice how neatly the double transition, namely, that of the intergrain junctions as well as that of the grains, is captured. We want to stress that their respective critical currents differ (see the inset) by a factor of 2×10^3. In this figure the well-defined slope (first linear portion) of CVC so often referred to in this paper is also clearly displayed. Note also

that CVC must be driven quite far in current to get a reliable slope, as for instance the slope in the large scale frame is about 20 times higher than the slope extracted from the inset (over the apparently linear portion). A linear behavior of V vs I with a temperature-independent slope above a certain current entails a progressive coincidence at any temperature between the differential resistance (dV/dI) and the absolute resistance (V/I) as current increases. Stated otherwise, at a high enough current level the measured resistance should saturate to a temperature-independent value. This is in fact what has been observed by some authors when studying the ''tail'' of the resistance transition $R(T)$ as a function of I in various families of copper oxide superconductors.[5]

There is a second linear regime [$I>5$ A in the example of Fig. 6(a)] that obviously should correspond with the whole sample gone normal. Both regimes are better visualized on a resistivity vs current plot as in Fig. 6(b). Here it is seen the two plateaus with well-defined resistivities, i.e., ohmic regimes, corresponding to the intergrain network and normal state, respectively. We have checked that indeed the higher resistivity value coincides quite well with the linear extrapolation of the normal-state resistivity to the actual temperature of 88.25 K.

The current dependence of the apparent integrain network resistivity for the three samples analyzed here is plotted in Fig. 7(a). Since (resistivity) saturation is reached at a different rate for the various samples (different critical currents, etc.) we have given the figure a uniform look by scaling each sample's current density differently. As an example, for sample Y16D2a of Fig. 6(b), the current density as plotted in Fig. 7 has been normalized by 225 A cm^{-2}. This procedure does not obviously change the saturation values of ρ_p. These three samples, whose main relevant parameters are shown in Table I, were chosen from a larger batch as representatives of low, medium, and high intergrain resistivities $\rho_{\rm wl}$ as given in the table. Note that indeed a factor of 20 separates the extreme values of $\rho_{\rm wl}$. Also shown are the normal-state percolative factor α_n, and the normal-state zero-intercept resistivity $\rho_n(0)$. Both α_n and $\rho_{\rm wl}$ have been calculated from the measured $\rho_n(0)$ and ρ_n' using Eqs. (3) and (4). The central point here is that according to our results in Secs. II and III, the normal-state intercept resistivity $\rho_n(0)$ times the anisotropy factor f should coincide with the paracoherent resistivity ρ_p. The fifth column of Table I shows the product for a value of $f=1/3$ as argued above. Finally, the last column displays the experimental values for ρ_p. As may be seen predicted values for ρ_p agree with experimental data within 20% and, even as importantly, with no free parameters. In fact, we believe that the comparison could be still improved if we knew the aspect ratio of the grains for each of the three samples [cf. Eq. (12)].

Figure 7(b), a graphic version of the same comparison, is a plot of the ratio of the experimental resistivity ρ to the product of the zero-intercept resistivity $\rho_n(0)$ and the anisotropy factor f. For current high enough to reach the ohmic regime, we see how the resistivity of the samples converges to $f\rho_n(0)$, i.e., their plotted ratio goes to 1. The dashed band in the figure corresponds to the extreme values of 0.28–0.38 for f, the central value taken as 1/3, associated with grain aspect ratios between 2.5–4.5 (see left vertical axis). The

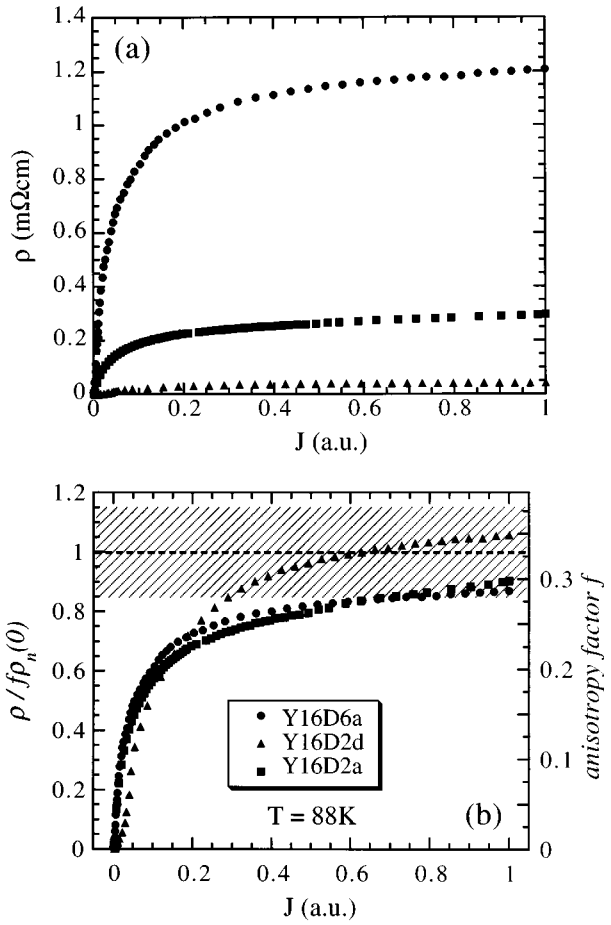

FIG. 7. (a) Resistivity for our three granular samples as a function of current density obtained from their current-voltage characteristics [cf. Fig. 6(b)]. For easier comparison, a scaling factor has been applied to the current density values of each sample (see text). (b) Same curves normalized by the intercept resistivity $\rho_n(0)$ times the anisotropy factor f. The observed convergence towards 1 for all samples is a no-free-parameter validation of our analysis. The dashed band covers the limiting values of f corresponding to extreme aspect ratios of grains.

excellent agreement is a graphical representation of the last two columns in Table I.

It is useful to get back to the intergrain resistivity $\rho_{\rm wl}$ and its connection with ρ_p. The experimental validation of the relationship $\rho_p=f\rho_n(0)$ provided in Table I is formally equivalent to the equality $\rho_p=\rho_{\rm wl}/\alpha_{\rm str}$ in Eq. (5). We can then put into numbers the error involved in the identification of ρ_p with $\rho_{\rm wl}$. For the three samples in Table I, $\rho_{\rm wl}$ differs from ρ_p by factors of 3.2, 4.7, and 2.6, respectively. A partial conclusion is that unless such an error is acceptable the intergrain resistivity cannot be determined solely from measurements below the critical temperature of the grains, i.e., in the paracoherent state. Formally, above the critical temperature of the grains ρ_n' and $\rho_n(0)$ are the data available to determine the two unknowns α_n and $\rho_{\rm wl}$ [see Eq. (4)]. On the contrary, below that temperature, only ρ_p is a datum for the two unknowns $\rho_{\rm wl}$ and $\alpha_{\rm str}$ [see Eq. (5)].

V. CONCLUSIONS

This paper has addressed the physical meaning of the well-defined resistivity ρ_p measured from the current-voltage

characteristics of granular high-temperature superconductors [see for instance Fig. 6(b)]. As advanced in the Introduction, arguments have been provided against identification used by different groups of ρ_p with the more physically relevant average intergrain resistivity ρ_{wl}. The (average) intergrain resistivity ρ_{wl} is not accessible from the ''superconducting'' state in spite of only intergrain boundaries being normal, but, paradoxically, it is accessible from the normal-state side. Furthermore we have shown that the apparent intergrain resistivity ρ_p is also predictable (within about 20%) from the normal-state resistivity with no free parameters involved. In concrete terms, for nontextured $YBa_2Cu_3O_{7-\delta}$ samples ρ_p come out to be one-third of the normal-state intercept resistivity. An explanation for this fact has been put forward based on the analysis of the percolative processes taking place in electrical conduction in granular media. As an intermediate result we have derived the resistivity enhancement due to anisotropy in randomly oriented granular samples using the approach of the effective-medium theory. Within the scope of the analysis here, simultaneous measurements of normal-state and paracoherent-state resistivities could provide an effective and quick measure for the degree of texturization (factor f) of grains in polycrystalline samples, but this issue is left for future work.

ACKNOWLEDGMENTS

This work has been supported by the Comisión Interministerial de Ciencia y Tecnología (MAT95-0279). A.D. acknowledges financial support from the Xunta de Galicia.

[1] See, e.g., R. Meisels, S. Bungre, and A. D. Caplin, J. Less Common. Met. **151**, 83 (1989); Y. S. Hascicek and L. R. Testardi, Phys. Rev. B **43**, 2853 (1991).

[2] See, e.g., A. C. Rose-Innes, in *Introduction to Superconductivity* (Pergamon, Oxford, 1969), Chap. 13.

[3] D. Goldschmidt, Phys. Rev. B **39**, 9139 (1989).

[4] S. S. Bungre, R. Meisels, Z. X. Shen, and A. D. Caplin, Nature (London) **341**, 725 (1989).

[5] W. C. McGinnis, T. E. Jones, E. W. Jacobs, R. D. Boss, and J. W. Schindler, IEEE Trans. Magn. **25**, 2138 (1989); M. Prester, E. Babic, M. Stubicar, and P. Nozar, Phys. Rev. B **49**, 6967 (1994).

[6] E. Babic, M. Prester, D. Babic, P. Nozar, P. Stastny, and F. C. Matacotta, Solid State Commun. **80**, 855 (1991).

[7] See, e.g., A. C. Wright, K. Zhang, and A. Erbil, Phys. Rev. B **44**, 863 (1991); T. B. Doyle and R. A. Doyle, *ibid*. **47**, 8111 (1993).

[8] J. W. Ekin, A. I. Braginski, A. J. Panson, M. A. Janocko, D. W. Capone, N. J. Zaluzec, B. Flandermeyer, O. F. de Lima, M. Hong, J. Kwo, and S. H. Liou, J. Appl. Phys. **62**, 4821 (1987).

[9] See, e.g., T. A. Friedmann, M. W. Rabin, J. Giapintzakis, J. P. Rice, and D. M. Ginsberg, Phys. Rev. B **42**, 6217 (1990).

[10] J. Halbritter, Int. J. Mod. Phys. B **3**, 719 (1989).

[11] J. Kirtley, Y. Imry, and P. K. Hansma, J. Low Temp. Phys. **17**, 247 (1974).

[12] J. Halbritter, M. R. Dietrich, H. Küpfer, B. Runtsch, and H. Wühl, Z. Phys. B **71**, 411 (1988).

[13] J. A. Veira and F. Vidal, Physica C **159**, 468 (1989).

[14] A. Díaz, A. Pomar, G. Domarco, J. Maza, and F. Vidal, Appl. Phys. Lett. **63**, 1684 (1993); J. Appl. Phys. **77**, 765 (1995).

[15] E. Babic, M. Prester, Z. Marohnic, T. Car, N. Biskup, and S. A. Siddiqui, Solid State Commun. **72**, 753 (1989).

[16] See, e.g., B. Batlogg, in *Physics of High-Temperature Superconductors*, edited by S. Maekawa and M. Sato (Springer-Verlag, Berlin, 1992), p. 219.

[17] P. Peyral, A. Raboutou, C. Lebeau, and J. Rossenblatt, J. Phys. C **20**, L155 (1987); M. Ashkin and M. R. Beasley, IEEE Trans. Magn. **23**, 1367 (1987).

[18] D. J. Bergmann and D. Stroud, in *Solid State Physics: Advances in Research and Applications*, edited by H. Ehrenreich and D. Turnbull (Academic, San Diego, 1992), Vol. 46; D. Stroud, Phys. Rev. B **12**, 3368 (1975).

[19] L. D. Landau and E. M. Lifshitz, *Course of Theoretical Physics* (Pergamon, Oxford, 1963), Vol. 8, Chap. 1, Sec. 4.

[20] See, e.g., J. W. Ekin, in *Processing and Properties of High-T_c Superconductors*, edited by S. Jin (World Scientific, Singapore, 1993), Vol. 1.